Maximized cooling efficiency for a Zeeman slower operating at optimized magnetic field profile

Zhuanxian Xiong (熊转贤)[1,2], Yun Long (龙 云)[1,2], Huixing Xiao (肖辉星)[1,2], Xi Zhang (张 曦)[1,2], Lingxiang He (贺凌翔)[1], and Baolong Lü (吕宝龙)[1*]

[1]*State Key Laboratory of Magnetic Resonance and Atomic and Molecular Physics, Wuhan Institute of Physics and Mathematics, Chinese Academy of Sciences, Wuhan 430071, China*

[2]*Graduate University of the Chinese Academy of Sciences, Beijing 100049, China*

[*]*Corresponding author: baolong_lu@wipm.ac.cn*

Received June 17, 2010; accepted August 20, 2010; posted online January 1, 2011

We build a Zeeman slower with consecutive coils and use it to load an Yb magneto-optical trap (MOTs). Cooling efficiency is measured by the fluorescence intensity of the atomic cloud trapped by the MOT. An optimized magnetic field profile can acquire the maximum cooling efficiency, corresponding to a good compromise between the smaller magnetic field mismatch and the high capture velocity. Our studies provide useful information on how the performance of the Zeeman slower can be improved.

OCIS codes: 020.3320, 020.7010, 020.7490.
doi: 10.3788/COL201109.010201.

The Zeeman slower was first developed by Phillips *et al*. in 1982[1]. It is more effective in creating slow atomic beams than other methods based on frequency chirping[2], frequency sweeping[3], broadband lasers[4−6], and so on. It has been widely used as a pre-cooling stage in magneto-optical traps (MOTs). Certain metal elements employed in optical clocks, such as Sr and Yb[7−14], which have very low vapor pressures at room temperature, cannot be trapped directly by a MOT. In such a case, a Zeeman-slowed atomic beam is usually the only choice to obtain a high flux of slow atoms for subsequent laser cooling. To produce the desired magnetic field profile, a tapered coil is normally adopted in a Zeeman slower[1,15]. It needs only one current supply; however, the magnetic coil requires precise design and construction for the optimal performance. Recently, a Zeeman slower based on magnetic dipoles and composed of an array of compact discrete neodymium magnets was proposed by Ovchinnikov[16,17]. This slower needs no current; however, it has the same limitations as the tapered coils. Dedman *et al*. performed detailed theoretical calculations of the magnetic field profile for a slowing light beam with non-uniform intensity distributions. Generally, precisely determining the optimal magnetic field profile is difficult because atomic cooling depends upon many other factors, such as the alignment and the spatial distribution of the slowing light beam. A novel type of Zeeman slower with consecutive coils was first demonstrated by Harris[18]. Although independent current controls for each coil make this system quite complicated, it is simpler to build. More importantly, it provides flexibility to optimize the magnetic field profile to acquire maximized cooling efficiency.

In this letter, we investigate how to improve the cooling efficiency of a Zeeman slower by considering the imperfection of its magnetic field distribution. We use a Zeeman slower made of consecutive coils to load an Yb MOT. The cooling efficiency of the Zeeman slower is increased by optimizing the magnetic field distribution. We first give a brief introduction of the principle of a Zeeman slower, and then provide a description of our Zeeman slower, as well as an analysis to the effect of the magnetic field distribution. We also present experimental observations to support our analysis.

In a Zeeman slower, a red-detuned laser beam is guided to counter-propagate against the atomic beam. A spatially varying magnetic field produces a varying Zeeman shift to compensate the changing Doppler shift of the atoms. The radiation force acting on an atom is given by[15]

$$F = \frac{\hbar k \Gamma}{2} \left(\frac{s(z)}{1 + s(z) + 4\Delta_{\rm eff}^2/\Gamma^2} \right), \tag{1}$$

where $\hbar$ is the Plank's constant divided by 2π, k is the wave vector, Γ is the linewidth of transition, $s(z)$ is the local saturation parameter along the axis of Zeeman slower, and $\Delta_{\rm eff} = \delta_0 + kv(z) - \mu' B(z)/\hbar$ is the effective detuning, which includes both the Doppler shift and the Zeeman shift. Here, δ_0 is the laser detuning, $v(z)$ is the velocity of the atoms, and μ' is the magnetic moment. If a moving atom is in resonance with the slowing laser (i.e., $\Delta_{\rm eff} = 0$), the magnetic field distribution $B(z)$ of the Zeeman slower can be written as

$$B(z) = \frac{\hbar}{\mu'} \left(\delta_0 + \frac{v(z)}{\lambda} \right), \tag{2}$$

where λ is the wavelength of the slowing laser. According to Eq. (1), the maximum deceleration rate $a_{\rm max} = \hbar k \Gamma / 2m$ (m is the atomic mass) can only be reached in the resonant case and at infinite intensity of the laser light. In practice, only a fraction of the maximum deceleration rate, $a = \eta\ a_{\rm max}$, is used in the design of a slower. Thus, a higher maximum velocity $v_{\rm max}$ requires a higher peak magnetic field to compensate for the larger Doppler shift. The distance over which slowing takes place is simply given by $L = (v_{\rm max}^2 - v_{\rm f}^2)/(2a)$, where $v_{\rm f}$ is the desired final velocity at the exit of the slower. The velocity as a

function of z takes the following form:

$$v_z = \sqrt{(1 - z/L)v_{\max}^2 + (z/L)v_{\rm f}^2}. \quad (3)$$

Thus, the desired spatial profile of the magnetic field is completely determined by Eqs. (2) and (3).

We built a slower for Yb, a metal element possessing a strong $^1S_0 - {}^1P_1$ transition ($\Gamma = 2\pi\times$ 29 MHz) at 398.9 nm, which is suitable for Zeeman slowing. The slower was made of 13 consecutive cylindrical coils. The coils were designed to carry different currents to create the required magnetic-field distribution along the axis of the slower. Each coil had 260 windings of copper wire and a current controlled independently by a homemade 13-way current source. The length of the slower was 26 cm, and a deceleration rate $a = 0.4a_{\max}$ was chosen for the design. The slower was thus able to capture atoms with initial velocities of up to 310 m/s. We first programmed independent calibration system for each coil by measuring its magnetic field distribution when only the single coil carried an electric current, whereas all other coils were shut off. If all the coils were switched on, their magnetic fields would be superimposed together to form an overall distribution over the slowing distance. Then, we used a fitting program to obtain the required current values of the coils that would produce an actual magnetic field distribution with the best match to the desired profile.

Figure 1(a) displays the desired magnetic field profiles and the actual magnetic field profiles produced by the slower. The upper dashed curve represents the initial design we intended to use in the experiment. The figure shows a peak magnetic field of approximately 341 Gs at the entrance of the slower, corresponding to a deceleration process at which the velocity decreases from 310 m/s to approximately 7 m/s over the whole effective slowing distance. There is a good agreement between the actual and desired field profiles. Nevertheless, we checked the residual small mismatch between these two curves. Figure 1(b) displays the amplitude difference of the actual and the desired fields, which shows a ripple-like fluctuation with the maximum amplitude of about 6 Gs. In the consecutive coil structure, the coil strength, which is defined as the product of the turns and current, does not vary smoothly along the z coordinate. As a result, the spatial profile of magnetic field is not smooth either, especially in the region between two adjacent coils. This imperfection in the actual magnetic field is unavoidable even if every coil has an ideal cylindrical shape, and is thus a disadvantage compared with tapered-coil Zeeman slowers. Although the field mismatch can be somewhat reduced by using more coils of smaller width, this method requires a more complicated electric current source. The deviation of the actual magnetic field from the ideal curve leads to a non-zero $\Delta_{\rm eff}$, which in turn results in a reduction of the radiation force F, according to Eq. (1). Apparently, F is more sensitive to $\Delta_{\rm eff}$ at smaller saturation parameters s. The slowing light we used is below the saturation intensity ($I_{\rm s} = 58$ mW/cm^2), corresponding to an average saturation parameter $s \approx 0.67$. Specifically, the amplitude of field fluctuation in Fig. 1(b) may cause a reduction of the radiation force by nearly 17%. The considerable change in the radiation force experienced by the atoms affects the slowing process in two ways. Firstly,

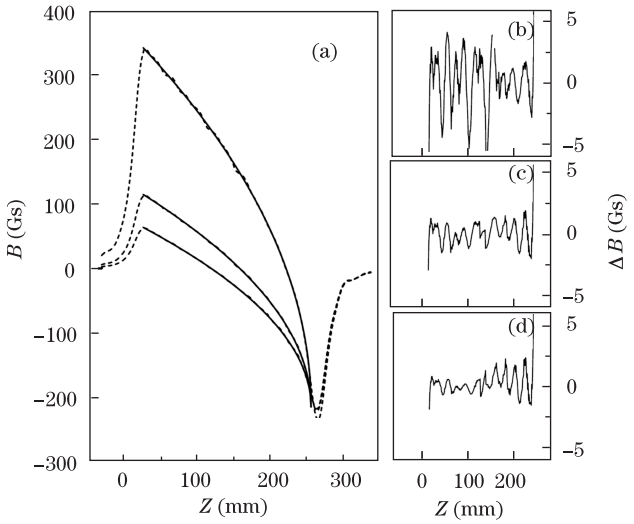

Fig. 1. (a) Magnetic field distribution of the Zeeman slower for Yb atoms. The solid and dashed lines represent the measured data and theoretical curves, respectively. The three pairs of curves, from top to bottom, correspond to a peak magnetic field of 341, 114, and 63 Gs, respectively. (b), (c), and (d) Deviation of the measured data with respect to the smooth theoretical curves for the three cases in (a), showing ripple-like fluctuations.

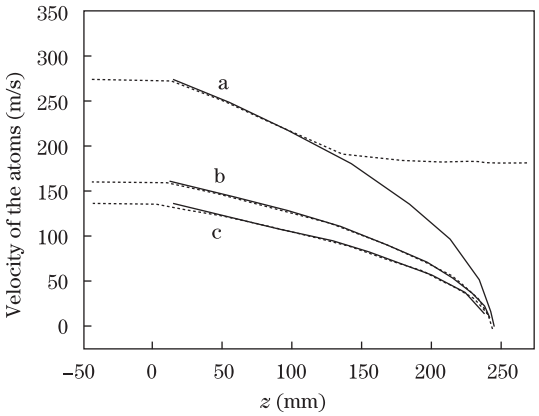

Fig. 2. Velocity versus position for atoms in the Zeeman slower. Curves a, b, and c correspond to the cases with a peak magnetic field of 341, 114, and 63 Gs, respectively, as in the case of Fig. 1. Solid lines represent designed velocities, whereas dashed lines represent calculated velocities when the fluctuation of the magnetic field is considered. Evidently, at lower B-field range, the deceleration process is less affected by the fluctuation of the magnetic field.

the atomic velocity cannot reach the desired value $v(z)$ due to the decreased deceleration rate. Secondly, the mismatch between the actual velocity and the desired velocity increases the effective detuning $\Delta_{\rm eff}$ due to the additional Doppler shift, which in turn causes a further decrease in the radiation force. Eventually, the atoms leave the slower at a higher velocity than the designed final velocity $v_{\rm f}$, as illustrated by the curve a in Fig. 2.

The discussion above implies that the imperfection in the magnetic field distribution somehow needs to be alleviated. Intuitively, the field mismatch should become smaller as the overall amplitude of the magnetic field is decreased. For example, the middle and bottom curves in Fig. 1(a) shows two magnetic field profiles, each with

a much lower peak field than the upper pair of curves. The corresponding magnetic field fluctuations are shown in Figs. 1(c) and (d), respectively. Compared with the case in Fig. 1(a), the fluctuation amplitudes are significantly reduced to a value less than 2 Gs. The cooling efficiency of the slower increases at lower fields. However, one has to bear in mind that the capture velocity $v_{\max}$ of the slower decreases when the peak magnetic field is reduced. A decline in the flux of the slow atoms thus occurs accordingly. Therefore, a good compromise between the capture velocity and the small magnetic field mismatch must be sought. This can be easily performed in the experiment by simply changing the magnetic field distribution.

In order to obtain cold Yb atoms, we built a MOT to trap the slowed atoms coming out of the Zeeman slower described above. The fluorescence signal of the MOT, which is proportional to the trapped atom number, may be regarded as a measure of the cooling efficiency of the slower. In other words, the more atoms the MOT collects, the more efficient the slower becomes. Our aim here is to observe the possible change in the cooling efficiency when the magnetic field distribution varies, to optimize the operation of the slower in the way discussed previously.

The experimental setup is sketched in Fig. 3. The setup consisted mainly of an oven, the Zeeman slower, and the MOT vacuum chamber. The temperature of the oven was kept at approximately 400 °C. The required blue light at the wavelength of 398.9 nm was delivered by a commercial laser (Toptica TA-SHG). Approximately 10 mW of the light was 300 MHz red-shifted by an acousto-optic modulator (AOM), which served as the slowing beam of the Zeeman slower. Another light beam of several milliwatts was guided to cross the atomic beam at a right angle. The induced fluorescence signal, nearly Doppler-free spectrum of atomic transitions, was used to calibrate the laser frequency. Three pairs of light beams with a total power of 50 mW and a beam diameter of 1 cm were used as the trapping beams of the MOT. Part of the fluorescence emitted by the atomic cloud was collected by an optical lens, and then sent to a photomultiplier tube (PMT). The sensitivity of the PMT to blue light was calibrated for the calculation of the trapped-atom number. A charge-coupled device (CCD) camera was placed in the opposite direction to record the fluorescence image of the atom cloud.

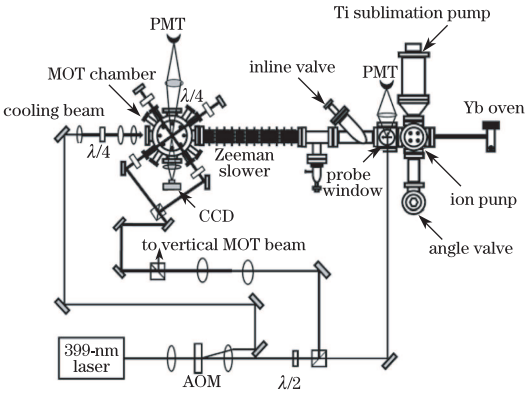

Fig. 3. Diagram of our Yb MOT apparatus with a multi-coil Zeeman slower.

Although our slower was designed for one isotope ^{174}Yb, the magnetic field distribution generated was very similar to that required by other isotopes. This is because all the isotopes have the same amount of Zeeman shift, and their atomic mass values are close to each other. Thus, the deceleration rates to all isotopes are nearly identical with the same magnetic field profile. In addition, the $^1S_0$ – $^1P_1$ cooling cycle is not fully closed because an excited atom at $^1P_1$ state has a small branching ratio to other metastable states. This means that the Yb MOT can be rapidly built up and can reach the steady state in a short time scale, given by the lifetime (about 0.3 s) of the cooling cycle.

In the experiment, as the laser frequency was slowly scanned, the MOT signal of different isotopes appeared subsequently (see Fig. 4). The relative intensities of the group of peaks were due to different isotope abundances. The data in Fig. 4 were taken under the same experimental conditions, except for the magnetic field distribution of the slower. Figure 4(a) corresponds to a magnetic field profile, as displayed by the upper curve in Fig. 1(a). In this case, the designed peak field and capture velocity were 341 Gs and 310 m/s, respectively. The trapped atom number of isotope ^{174}Yb in the MOT was estimated to be 4.8×10^7. To check the performance of the slower with a smaller magnetic field fluctuation, we reduced the peak field to 114 Gs. The magnetic field then follows the profile of the middle curve in Fig. 1(a). Accordingly, the capture velocity was reduced to 183 m/s. Figure 4(b) displays the MOT signal in this situation for comparison. The atomic number of ^{174}Yb increased to 8×10^7, corresponding to approximately 67% enhancement compared with Fig. 4(a). All other isotopes acquired roughly the same amount of enhancement. We also measured the MOT signals for other peak field values; however, Fig. 4(b) gives the maximal signal acquired. The figure shows that the efficiency of the Zeeman slower can indeed be increased by reducing the mismatch of the magnetic field distribution. However, when the peak field was further reduced from 114 Gs, the MOT signal dropped instead. As an example, Fig. 4(c) shows a curve for a specific magnetic field profile described by the bottom curve in Fig. 1(a), for which the peak field and capture velocity were lowered to 63 Gs and 155 m/s, respectively. This indicates that the negative effect of the reduced atomic flux plays a more important role if the capture velocity is too small. Just as predicted before, the

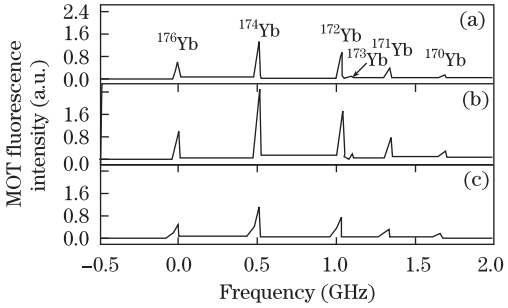

Fig. 4. Fluorescence signals of the MOT for different Yb isotopes as the laser frequency is scanned. The peak magnetic field of the Zeeman slower is, as in the case of Fig. 1(a), (a) 341, (b) 114, and (c) 63 Gs, respectively.

maximum efficiency of the slower can be acquired by making a compromise between the small magnetic field mismatch and high capture velocity.

In conclusion, a Zeeman slower with consecutive coils has been constructed and tested to provide the slow atom source for an Yb MOT. Our analysis shows that the mismatch between the actual and desired magnetic field distributions of the slower may impair the slowing process due to reduced deceleration rate, especially for magnetic field profiles with a high peak field. In the experiment, we record the fluorescence signal of the atom cloud trapped in the MOT as an actual measure of the cooling efficiency of the slower. Our observations prove that the cooling efficiency does not increase monotonically with increased peak field (and hence the increased capture velocity) because of the presence of magnetic field mismatch. Compared with the initial design, the trapped atom number is increased by approximately 67% at the optimized magnetic field profile of the Zeeman slower. Our results confirm that the performance of the Zeeman slower can be considerably improved by simply optimizing the magnetic field profile.

This work was supported by the National Natural Science Foundation of China (Nos. 10634060 and 10904161) and the National Key Basic Research and Development Program of China (Nos. 2005CB724501 and 2006CB921406).

References

1. W. D. Phillips and H. Metcalf, Phys. Rev. Lett. **48,** 596 (1982).
2. H. Wallis and W. Ertmer, J. Phys. B **21,** 2999 (1988).
3. R. Blatt, W. Ertmer, and J. L. Hall, Prog. Quantum Electron. **8,** 237 (1984).
4. M. Zhu, C. W. Oates, and J. L. Hall, Phys. Rev. Lett. **67,** 46 (1991).
5. Y. Shen, C. Gu, L. Xu, A. Wang, H. Ming, Y. Liu, and X. Wang, Chin. Opt. Lett. **7,** 1022 (2009).
6. S. Yan, J. Zhang, and W. Zhao, Chin. Opt. Lett. **6,** 676 (2008).
7. M. Takamoto, F.-L. Hong, R. Higashi, and H. Katori, Nature **435,** 321 (2005).
8. A. V. Taichenachev, V. I. Yudin, C. W. Oates, C. W. Hoyt, Z. W. Barber, and L. Hollberg, Phys. Rev. Lett. **96,** 083001 (2006).
9. Z. W. Barber, C. W. Hoyt, C. W. Oates, L. Hollberg, A. V. Taichenachev, and V. I. Yudin, Phys. Rev. Lett. **96,** 083002 (2006).
10. C. W. Hoyt, Z. W. Barber, C. W. Oates, T. M. Fortier, S. A. Diddams, and L. Hollberg, Phys. Rev. Lett. **95,** 083003 (2005).
11. I. Courtillot, A. Quessada, R. P. Kovacich, A. Brusch, D. Kolker, J.-J. Zondy, G. D. Rovera, and P. Lemonde, Phys. Rev. A **68,** 030501(R) (2003).
12. T. Hong, C. Cramer, E. Cook, W. Nagourney, and E. N. Fortson, Opt. Lett. **30,** 2644 (2005).
13. C. Y. Park and T. H. Yoon, Phys. Rev. A **68,** 055401 (2003).
14. A. D. Ludlow, M. M. Boyd, T. Zelevinsky, S. M. Foreman, S. Blatt, M. Notcutt, T. Ido, and J. Ye, Phys. Rev. Lett. **96,** 033003 (2006).
15. C. J. Dedman, J. Nes, T. M. Hanna, R. G. Dall, K. G. H. Baldwin, and A. G. Truscott, Rev. Sci. Instrum. **75,** 5136 (2004).
16. Y. B. Ovchinnikov, Opt. Commun. **276,** 261 (2007).
17. Y. B. Ovchinnikov, Eur. Phys. J. Special Topics **163,** 95 (2008).
18. M. L. Harris, "Design and construction of an improved Zeeman slower" Master Thesis (Duke University, Durham, 2003).